Supplementary Information for:

Fluorescence and Phosphorescence of Flavylium Cation Analogues of Anthocyanins

Gustavo T. M. Silva[1#], Cassio P. Silva[1#], Karen M. Silva[1,2], Renan M. Pioli[1], Tássia S. Costa[3], Vinícius V. Marto[3], Adilson A. Freitas[4], Jennifer Rozendo[1], Lucas M. O. S. Martins[1], Victor F. Cavalcante[1], Liuqing Sun[5], Adelia J. A. Aquino[5,6], Vânia M. T. Carneiro[3] and Frank H. Quina[1]*

[1] Instituto de Química, Universidade de São Paulo, Avenida Lineu Prestes 748, 05508-900, São Paulo, Brazil.

[2] Instituto Federal de Educação, Ciência e Tecnologia de São Paulo, 01109-010 São Paulo, Brazil.

[3] Departamento de Química, Universidade Federal de Viçosa, Avenida Peter Henry Rolfs s/n, Campus Universitário, 36570-900, Viçosa, Minas Gerais, Brazil.

[4] Instituto Superior Técnico, Universidade de Lisboa, 1049001, Lisbon, Portugal.

[5] School of Pharmaceutical Science and Technology, Tianjin University, Tianjin 300072, People's Republic of China.

[6] Department of Mechanical Engineering, Texas Tech University, Lubbock, TX 79409, USA.

[#] These authors contributed equally

*Corresponding author:

Frank H. Quina: quina@usp.br

Characterization data of the new compounds:

FL-9: 2-(4-iodophenyl)-5,7-dihydroxy-4-methylchromenium chloride

^{1}H NMR (500 MHz, Methanol-d_4 / 1% TFA– d_1): δ 8.11 – 8.06 (m, 5H), 7.00 (d, J = 2.2 Hz, 1H), 6.73 (d, J = 2.2 Hz, 1H). ^{13}C NMR (126 MHz, Methanol-d4 / 1% DCl): δ 172.7, 172.2, 168.3, 163.4, 160.5, 140.5, 130.6, 129.8, 117.6, 115.2, 114.7, 104.3, 96.7. HRMS, Calcd for $C_{16}H_{12}O_3I$ $[M\text{-}Cl]^+$ 378.9831; Found 378.9832.

FL10: 2-(4-bromophenyl)-5,7-dihydroxy-4-methylchromenium chloride

^{1}H NMR (500 MHz, Methanol-d_4 / 1% TFA– d_1): δ 8.26 – 8.23 (m, 2H), 8.11 (s, 1H), 7.89 – 7.86 (m, 2H), 7.00 (d, J = 2.2 Hz, 1H), 6.73 (d, J = 2.2 Hz, 1H). ^{13}C NMR (126 MHz, Methanol-d_4 / 1% DCl): δ 172.8, 172.2, 167.9, 163.4, 160.5, 134.3, 131.3, 131.1, 129.5, 115.4, 114.7, 104.3, 96.7. HRMS, Calcd for $C_{16}H_{12}O_3Br$ $[M\text{-}Cl]^+$ 330.9970; Found 330.9970.

FL14: 2-(3-bromo-4-methoxyphenyl)-7-methoxychromenium chloride

^{1}H NMR (500 MHz, Methanol-d_4/TFA) δ 9.26 (dd, J = 8.7, 0.8 Hz, 1H), 8.80 (d, J = 2.4 Hz, 1H), 8.58 (dd, J = 8.9, 2.4 Hz, 1H), 8.52 (d, J = 8.7 Hz, 1H), 8.24 (d, J = 9.0 Hz, 1H), 7.93 (dd, J = 2.4, 0.8 Hz, 1H), 7.58 (dd, J = 9.0, 2.4 Hz, 1H), 7.44 (d, J = 8.9 Hz, 1H), 4.19 (s, 3H), 4.12 (s, 3H). ^{13}C NMR (126 MHz, Methanol-d_4 / 1% DCl): δ 172.8, 171.4, 164.4, 161.1, 156.0, 135.5, 133.3, 133.1, 123.9, 123.3, 121.5, 114.9, 114.7, 114.5, 101.6, 58.3 , 57.9. HRMS, Calcd for $C_{17}H_{14}O_3Br$ $[M\text{-}Cl]^+$ 345.0126; Found 345.0130.

FL-15: 2-(3-bromo-4-methoxyphenyl)-7-hydroxy-4-methylchromenium chloride

^{1}H NMR (500 MHz, Methanol-d_4/TFA) δ 10.25 (d, J = 2.4 Hz, 1H), 10.05 (dd, J = 8.9, 2.4 Hz, 1H), 9.93 (s, 1H), 9.91 (d, J = 9.1 Hz, 1H), 9.08 (d, J = 2.3 Hz, 1H), 9.01 (dd, J = 9.2, 2.3 Hz, 1H), 8.95 (d, J = 8.9 Hz, 1H), 5.65 (s, 3H). ^{13}C NMR (126 MHz, Methanol-d_4/TFA) δ 170.5, 170.4, 170.3, 163.8, 160.0, 135.1, 132.3, 130.5, 123.8, 122.6, 120.3, 115.4, 114.5, 114.3, 103.8, 57.8. HRMS, Calcd for $C_{16}H_{12}O_3Br$ $[M\text{-}Cl]^+$ 330.9969; Found 330.9970.

FL-16: 2-(3-bromo-4-methoxyphenyl)-7-methoxy-4methylchromenium chloride

^{1}H NMR (500 MHz, Methanol-d_4/TFA) δ 10.33 (d, J = 2.4 Hz, 1H), 10.11 (dd, J = 8.9, 2.4 Hz, 1H), 10.05 (s, 1H), 9.95 (d, J = 9.3 Hz, 1H), 9.43 (d, J = 2.4 Hz, 1H), 9.12 (dd, J = 9.3, 2.5 Hz, 1H), 8.98 (d, J = 8.9 Hz, 1H), 5.73 (s, 3H), 5.67 (s, 3H).^{13}C NMR (126 MHz, Methanol-d_4/TFA) δ 170.9, 170.8, 170.7, 164.1, 160.0, 135.3, 132.6, 129.7, 123.7, 122.7, 121.0, 116.2, 114.6, 114.4, 101.7, 58.0, 57.8. HRMS, Calcd for $C_{18}H_{16}O_3Br$ $[M\text{-}Cl]^+$ 359.0283; Found 359.0283.

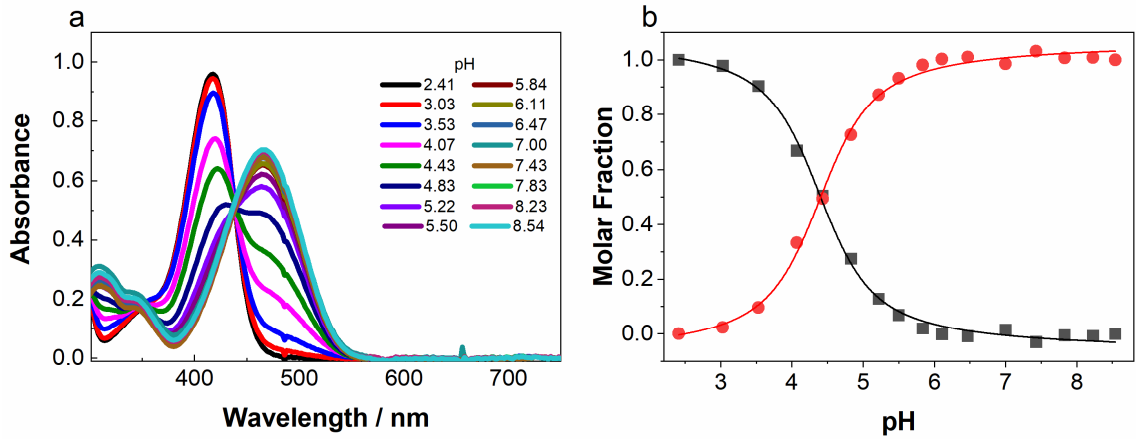

Figure S1. Determination of the pK_a of **FL2**: (a) spectral changes as a function of pH within 5 s; (b) decrease in the fraction of $\mathbf{AH^+}$ (black) and increase in **A** (red).

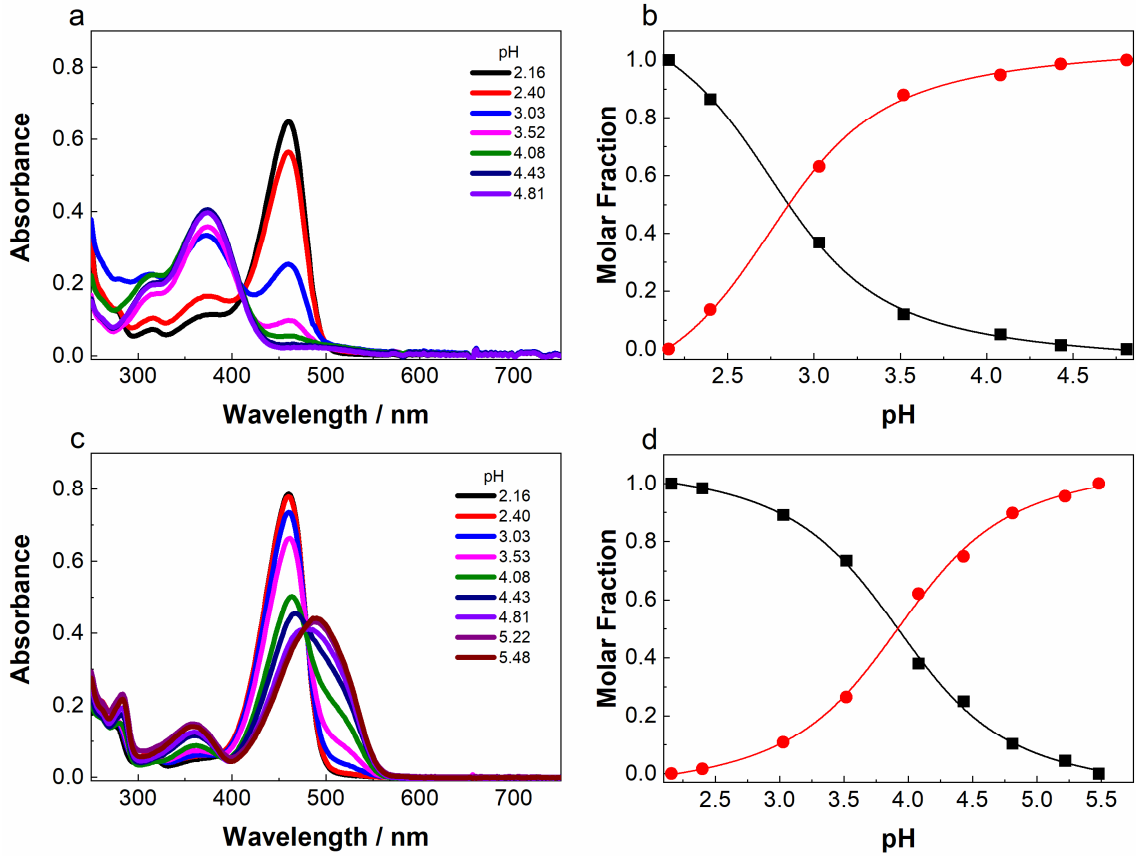

Figure S2. Determination of the pK_{ap} of **FL3**: (a) spectral changes as a function of pH after 24 h; (b) decrease in the fraction of $\mathbf{AH^+}$ (black) and increase in the other forms (red). Determination of the pK_a of **FL3**: (c) spectral changes as a function of pH within 5 s; (d) decrease in the fraction of $\mathbf{AH^+}$ (black) and increase in **A** (red).

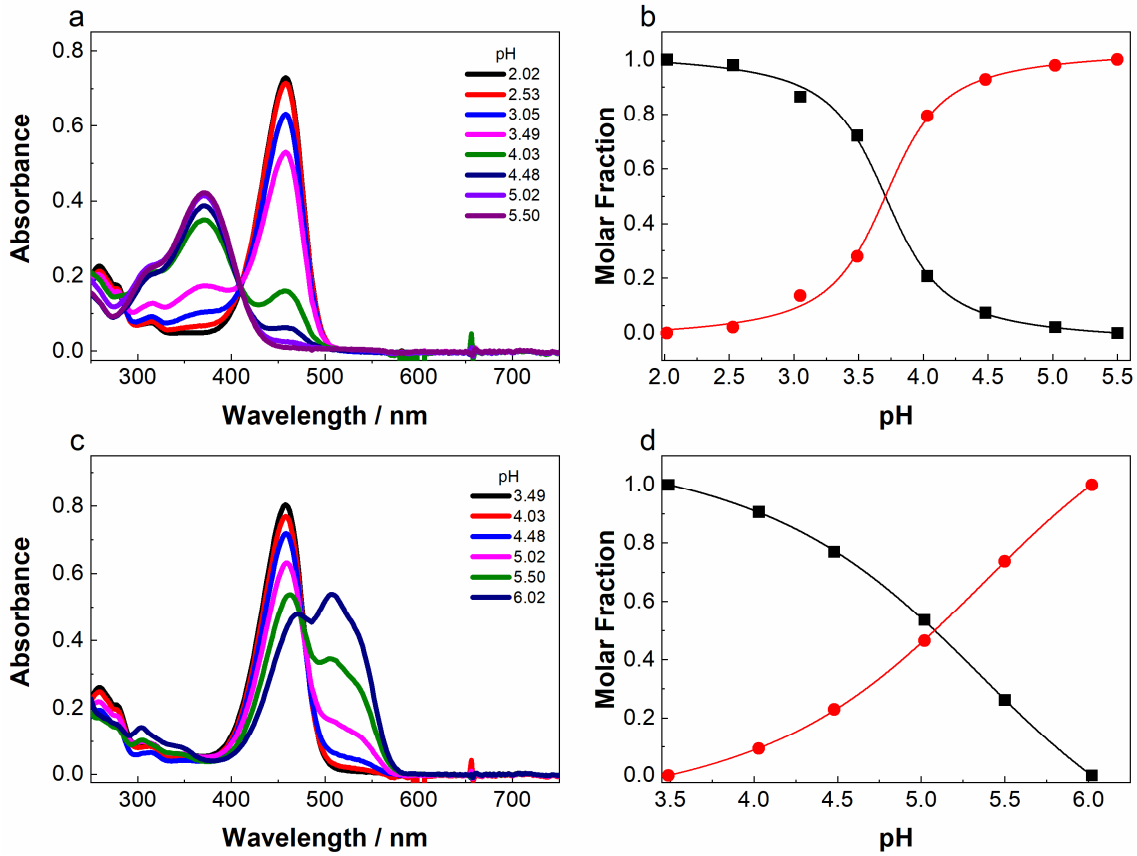

Figure S3. Determination of the pK_{ap} of **FL4**: (a) spectral changes as a function of pH after 24 h; (b) decrease in the fraction of $\mathbf{AH^+}$ (black) and increase in the other forms (red). Determination of the pK_a of **FL4**: (c) spectral changes as a function of pH within 5 s; (d) decrease in the fraction of $\mathbf{AH^+}$ (black) and increase in **A** (red).

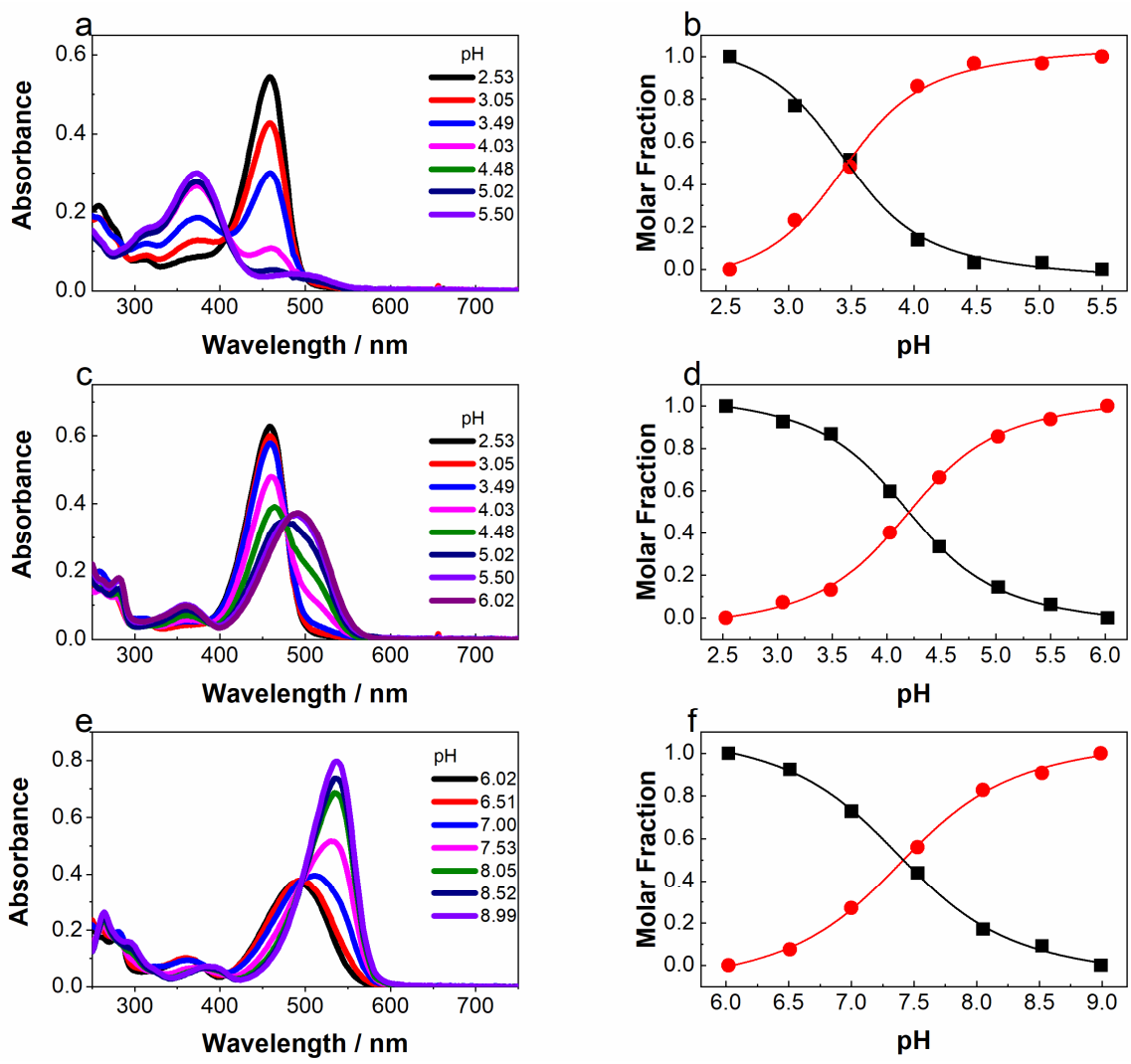

Figure S4. Determination of the pK_{ap} of **FL5**: (a) spectral changes as a function of pH after 24 h; (b) decrease in the fraction of $\mathbf{AH^+}$ (black) and increase in the other forms (red). Determination of the first and second pK_as of **FL4**: (c,e) spectral changes as a function of pH within 5 s; (d) decrease in the fraction of $\mathbf{AH^+}$ (black) and increase in **A** (red); (f) decrease in the fraction of **A** (black) and increase in $\mathbf{A^-}$ (red).

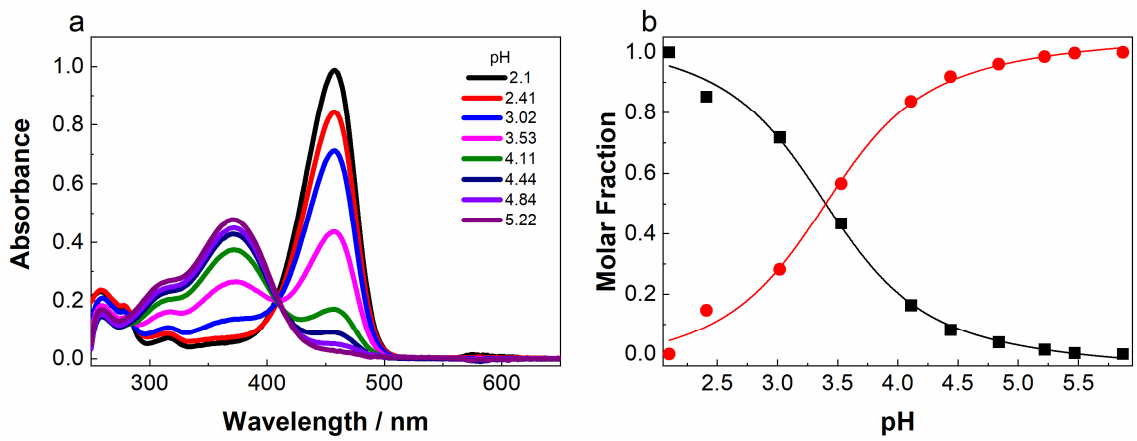

Figure S5. Determination of the pK_{ap} of **FL6**: (a) spectral changes as a function of pH after 24 h; (b) decrease in the fraction of $\mathbf{AH^+}$ (black) and increase in the other forms (red).

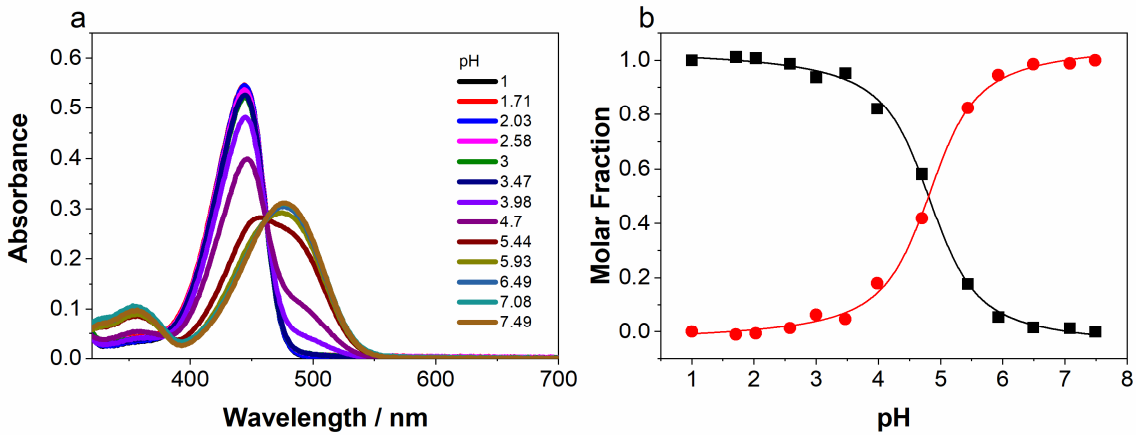

Figure S6. Determination of the pK_a of **FL7**: (a) spectral changes as a function of pH within 5 s; (b) decrease in the fraction of $\mathbf{AH^+}$ (black) and increase in **A** (red).

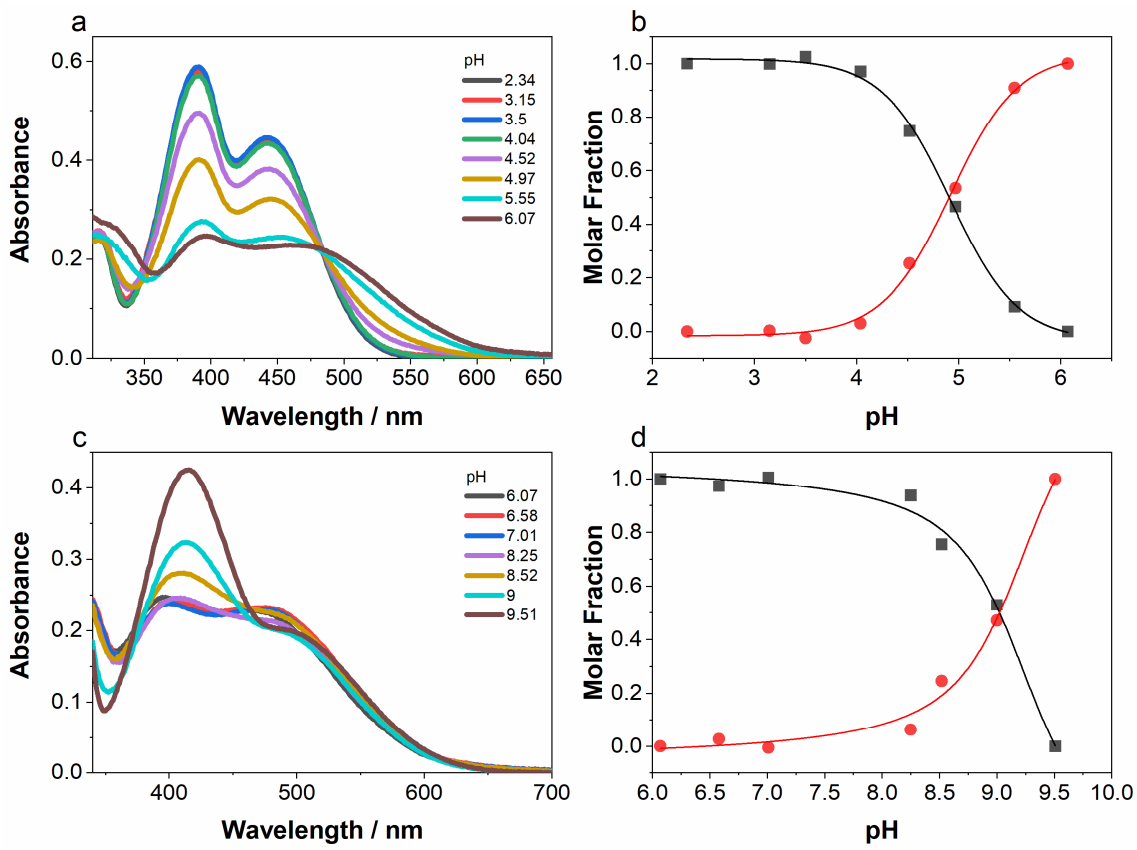

Figure S7. Determination of the first and second pK_as of **FL9**: (a,c) spectral changes as a function of pH within 5 s; (b) decrease in the fraction of $\mathbf{AH^+}$ (black) and increase in **A** (red); (d) decrease in the fraction of **A** (black) and increase in $\mathbf{A^-}$ (red).

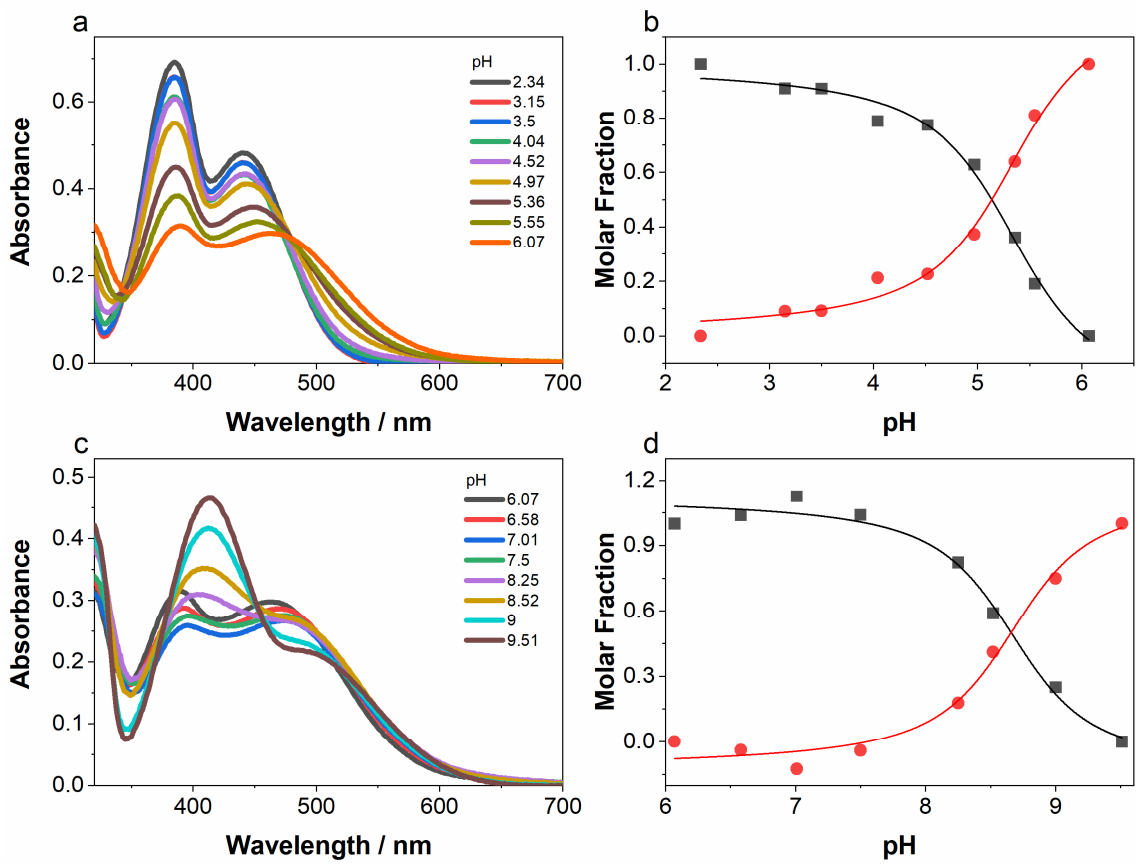

Figure S8. Determination of the first and second pK_as of **FL10**: (a,c) spectral changes as a function of pH within 5 s; (b) decrease in the fraction of $\mathbf{AH^+}$ (black) and increase in **A** (red); (d) decrease in the fraction of **A** (black) and increase in $\mathbf{A^-}$ (red).

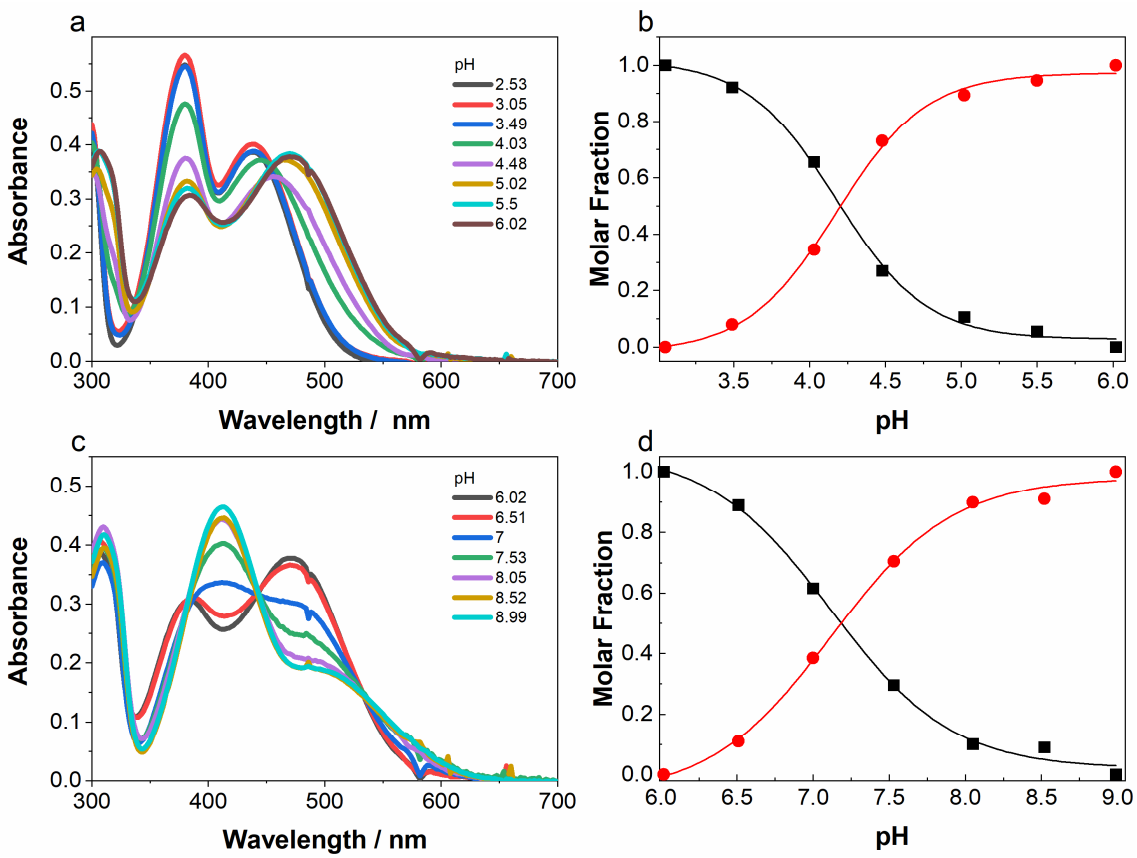

Figure S9. Determination of the first and second pK_as of **FL11**: (a,c) spectral changes as a function of pH within 5 s; (b) decrease in the fraction of $\mathbf{AH^+}$ (black) and increase in **A** (red); (d) decrease in the fraction of **A** (black) and increase in $\mathbf{A^-}$ (red).

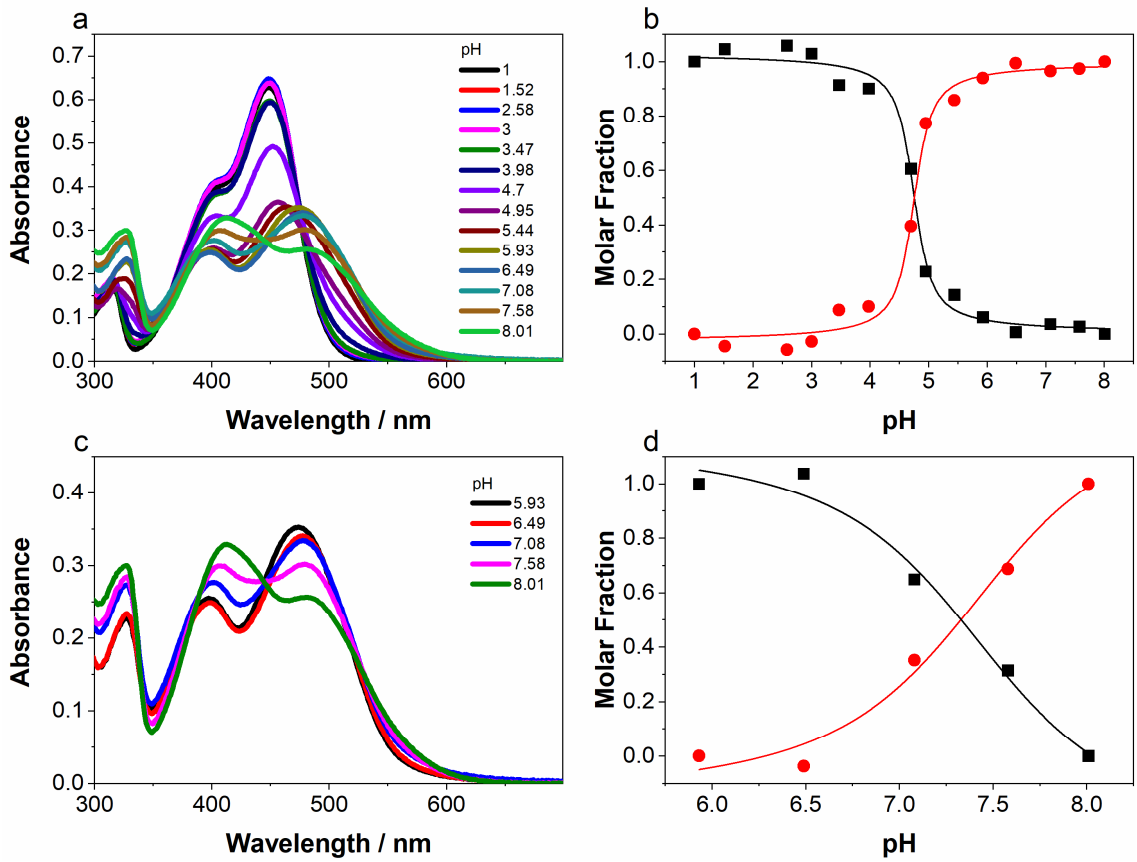

Figure S10. Determination of the first and second pK_as of **FL12**: (a,c) spectral changes as a function of pH within 5 s; (b) decrease in the fraction of $\mathbf{AH^+}$ (black) and increase in **A** (red); (d) decrease in the fraction of **A** (black) and increase in $\mathbf{A^-}$ (red).

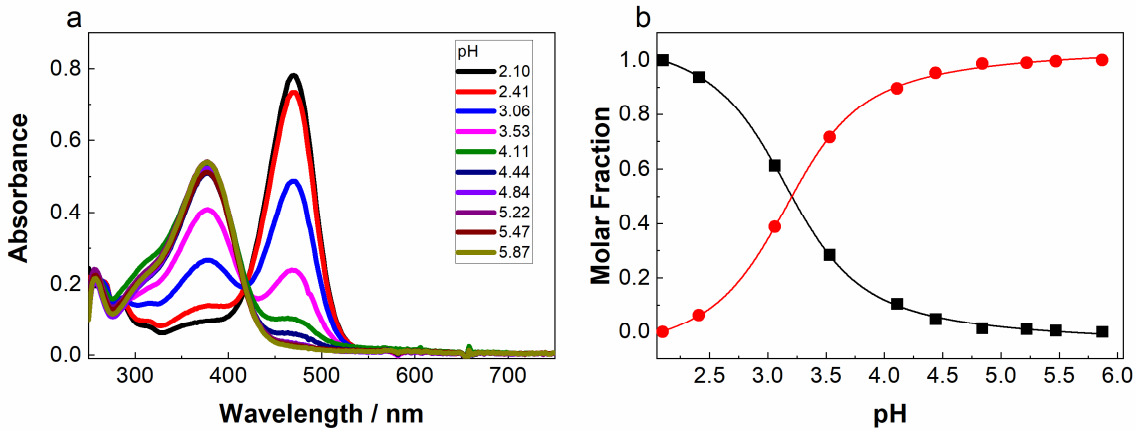

Figure S11. Determination of the pK_{ap} of **FL13**: (a) spectral changes as a function of pH after 24 h; (b) decrease in the fraction of $\mathbf{AH^+}$ (black) and increase in the other forms (red).

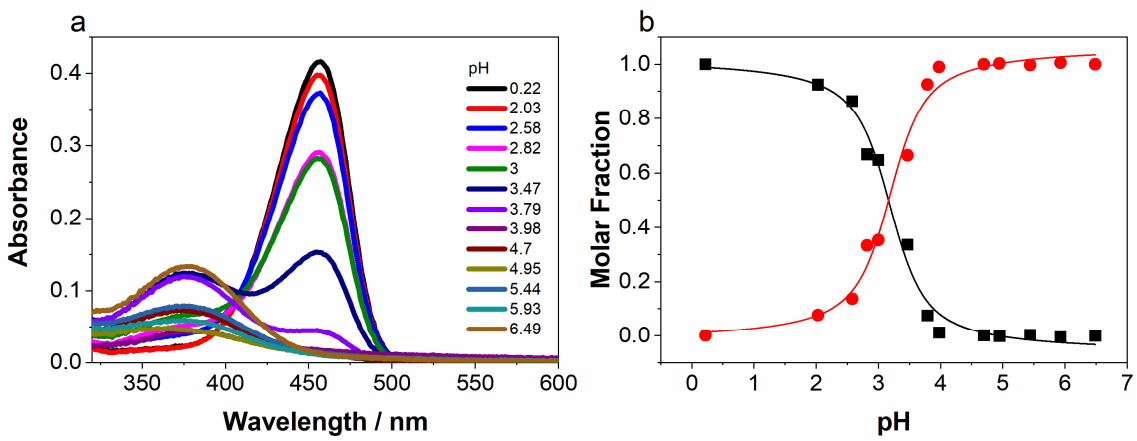

Figure S12. Determination of the pK_{ap} of **FL14**: (a) spectral changes as a function of pH after 24 h; (b) decrease in the fraction of $\mathbf{AH^+}$ (black) and increase in the other forms (red).

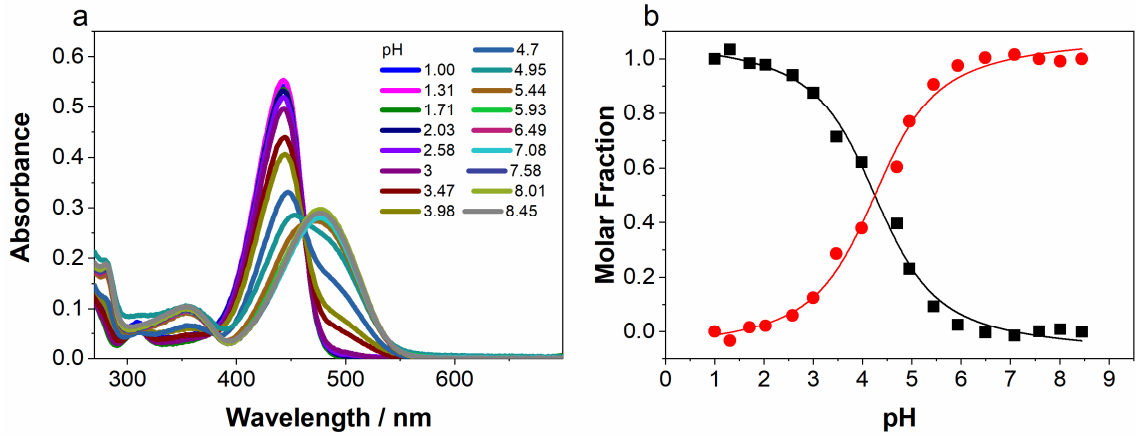

Figure S13. Determination of the pK_a of **FL15**: (a) spectral changes as a function of pH within 5 s; (b) decrease in the fraction of $\mathbf{AH^+}$ (black) and increase in **A** (red).

Table S1. Vertical excitation energies E (in eV and in nm), oscillator strength ***f*** and the charge transfer character q(CT) (in units of e) by ADC(2)/def2-TZVP in the gas phase and in COSMO acetonitrile of the five lowest energy excited singlet states of selected flavylium cations.

System	Excited state	Gas Phase			Acetonitrile		
		ΔE (eV/nm)	*f*	q(CT)	ΔE (eV/nm)	*f*	q(CT)
FL6	**S_1**	**2.62/474**	**0.85**	**0.48**	**2.67/465**	**0.87**	**0.42**
	S_2	3.31/374	0.02	0.31	3.34/371	0.03	0.31
	S_3	3.94/315	0.00	0.63	3.99/311	0.00	0.60
	S_4	4.16/298	0.05	0.29	4.18/297	0.08	0.35
	S_5	4.64/267	0.06	0.44	4.76/261	0.06	0.37
FL8	**S_1**	**2.67/464**	**0.82**	**0.46**	**2.73/455**	**0.84**	**0.45**
	S_2	3.34/371	0.03	0.34	3.37/368	0.04	0.33
	S_3	3.97/312	0.00	0.62	4.06/306	0.02	0.51
	S_4	4.16/298	0.07	0.30	4.18/297	0.10	0.38
	S_5	4.69/264	0.05	0.46	4.80/258	0.05	0.36
FL12	**S_1**	**2.67/464**	**0.75**	**0.46**	**2.74/452**	**0.73**	**0.41**
	S_2	3.03/409	0.04	0.30	3.09/402	0.09	0.33
	S_3	3.91/317	0.04	0.39	4.00/310	0.09	0.33
	S_4	3.97/312	0.04	0.58	4.02/308	0.02	0.62
	S_5	4.63/268	0.05	0.42	4.71/263	0.18	0.21
FL16	**S_1**	**2.62/473**	**0.75**	**0.53**	**2.75/451**	**0.80**	**0.42**
	S_2	3.29/377	0.01	0.35	3.37/368	0.04	0.34
	S_3	3.59/345	0.05	0.63	3.85/322	0.01	0.51
	S_4	4.15/299	0.07	0.29	4.19/296	0.12	0.37
	S_5	4.54/273	0.02	0.51	4.72/263	0.01	0.39
FL13	**S_1**	**2.44/508**	**0.67**	**0.55**	**2.62/474**	**0.85**	**0.45**
	S_2	3.10/400	0.10	0.48	3.30/376	0.02	0.36
	S_3	3.38/367	0.06	0.46	3.69/336	0.01	0.60
	S_4	4.14/300	0.04	0.29	4.16/298	0.08	0.34
	S_5	4.45/279	0.00	0.58	4.33/286	0.00	0.62

Table S2. ADC(2)/def2-TZVP vertical absorption and adiabatic and vertical fluorescence emission energies (eV) for the S_1 state and changes in the Ring-B/Ring-C dihedral angle between S_0 and S_1 in the gas phase

Flavylium Cation	Vertical absorption (eV/nm)	Adiabatic (eV/nm)	Vertical fluorescence emission (eV/nm)	Ring-B/Ring-C Dihedral angle in S_0 (degrees)	Increase of the Ring-B/Ring-C Dihedral angle in S_1 (degrees)
FL6	2.62/473	2.52/492	2.41/515	2.0	0.3
FL8	2.67/464	2.57/482	2.47/502	2.6	0.3
FL12	2.67/464	2.46/504	1.95/636	12.8	7.7
FL16	2.62/473	2.51/492	2.39/519	1.5	0.2
FL13	2.44/508	2.05/605	1.66/747	1.0	30